NUCLEAR ENGINEERING AND TECHNOLOGY
ISSN / eISSN 1738-5733
Publisher KOREAN NUCLEAR SOC,
NUTOPIA BLDG, 342-1 JANGDAE-DONG, DAEJEON,
SOUTH KOREA, 305-308,
Volume 26-Issue 1-(2026)
DOI:https://doi.org/10.65281/709946

OPEN ACCESS

FPGA Implementation Based on an Improved Defogging Algorithm: For Visual Monitoring Applications in Nuclear Engineering

Check for updates

Ruiyang Sang[1] Yuekai Zhu[2*] Junteng Wang[345]

1.Nanjing University of Information Science and Technology，

School of Computer Science、 School of Software

2.Universidad de Murcia；International Transdisciplinary Academic Congress

（ITAC）；Hong Kong Anmai Publishing

3.Shandong Youth University of Political Science

4.University of Newcastle

5.Singapore Graphic Science Press

Abstract: With the continuous advancement of computer vision systems, digital images and video have been widely adopted in all-scenario industrial measurement and control applications. However, under adverse environmental conditions such as smog, suspended atmospheric aerosol particles in the optical imaging path continuously absorb and scatter incident light, directly causing severe degradation in the image quality of panoramic images and real-time video across multiple dimensions,This gives rise to core imaging defects such as blurred image details, a sharp drop in dynamic contrast, and color distortion, severely disrupting critical operational workflows in high-end specialized industrial visual monitoring applications. These include comprehensive traffic monitoring and control, multidimensional surveillance and management of nuclear engineering sites, closed-loop visual inspections of reactor perimeters, and visual verification for comprehensive security at nuclear facilities.Visual monitoring scenarios specific to nuclear engineering have rigid technical requirements for high-level closed-loop coordination, high-fidelity imaging, microsecond-level low latency, and all-weather, uninterrupted continuous imaging.Natural fog and dust, combined with fine floating aerosol particles generated by equipment maintenance within the facility, interact to degrade the native image quality of front-end visual data, severely hindering the precise quantitative assessment of the facility's operational

status and the closed-loop maintenance operations required to trace and resolve anomalies across the entire site perimeter.Therefore, there is an urgent need to develop solutions specifically tailored to the multidimensional, demanding operational conditions of nuclear engineering. This requires targeted, highly efficient, adaptive defogging and image enhancement processing for low-quality, complex foggy images and videos, to losslessly restore high-definition native real-scene image quality and solidify the core foundation of embedded imaging computing power for comprehensive visual monitoring in nuclear engineering.Based on the specific scenarios of special industrial measurement and control in nuclear engineering, this paper conducts multi-dimensional, lightweight optimization and iteration of classic dark-channel prior-based defogging algorithms. It precisely meets the stringent technical requirements for on-site embedded systems in nuclear engineering—including low power consumption, millisecond-level real-time performance, and strong electromagnetic interference resistance—and integrates with on-site Field-Programmable Gate Array (FPGA) hardware platforms.it achieves a closed-loop processing workflow for directional, high-precision defogging and enhancement of real-world images and videos captured across the entire nuclear engineering site. This fully leverages the core hardware advantages of FPGAs—including parallel high-speed computing power, ultra-low power consumption, and compact on-board integration—to rapidly enable real-time defogging computing resource allocation for visual monitoring across all time periods and locations in nuclear engineering. It comprehensively addresses the critical need for on-site, embedded, and locally integrated deployment across all operational conditions.

Keywords: Image defogging; Computer vision systems; Digital images and video; FPGA hardware; Visual monitoring in nuclear engineering; All-weather imaging for plant site inspections

Foreword

With the comprehensive iterative upgrades in computer vision measurement and control technology, high-definition digital images and real-time video have achieved full coverage across all core industrial measurement and control scenarios. This has significantly empowered cutting-edge technological fields across the board, including precision medical diagnostics, comprehensive national defense and security, intelligent

traffic analysis, multidimensional target identification, comprehensive intelligent security monitoring, and closed-loop verification of high-risk industrial sites.In particular, within the comprehensive closed-loop safety production management system for nuclear engineering, round-the-clock, comprehensive visual monitoring serves as the essential technological foundation for core equipment security and maintenance, detailed inspections of plant-wide operational conditions, and comprehensive risk control at high-risk perimeter zones.Relying entirely on high-definition, low-latency real-time imagery and video, the system enables 24/7, blind-spot-free closed-loop monitoring and intelligent verification of peripheral pressure-bearing facilities surrounding nuclear reactors, closed-loop zones for physical isolation of radioactive zones, and high-risk dynamic work sites within the plant.The image quality and precision of native front-end visual imaging directly determine the efficiency of rapid identification of latent on-site hazards across the nuclear engineering facility, the accuracy of predictive quantification of critical electromechanical equipment failures, and the overall reliability of comprehensive, closed-loop security management across the entire facility.In the global industrial measurement and control sector, technical thresholds for front-end, in-situ image and video acquisition with native, high-fidelity image quality and real-time transmission computing power continue to rise incrementally. Leveraging multi-dimensional, effective feature information from high-definition digital images, core challenges in complex industrial production and maintenance operations have been efficiently resolved. Digital image processing technology has now become an indispensable core support technology in high-end industrial research and comprehensive safety production and maintenance systems.However, the end-to-end collection of images and video at the front end is highly susceptible to interference from extreme weather conditions. In complex environments such as widespread fog, severe smog, heavy rainfall, blizzards, and dust accumulation, the native image and video data suffer irreversible and severe degradation in image quality, failing to meet the basic standards for routine safety production and operations in high-end nuclear industrial scenarios.The core causes of

complex fog conditions include multi-dimensional coupled factors such as the condensation and aggregation of natural water vapor across the entire area, the dispersion of fine particulate dust from routine operations within industrial sites, and the accumulation of fine particulate matter in the atmosphere. In widespread haze conditions, high concentrations of ultrafine suspended dust particles are the primary cause of interference in optical imaging chains.Compared to conventional civilian outdoor visual monitoring scenarios, the specialized conditions within enclosed nuclear engineering facilities—in addition to widespread natural haze interference—are compounded by micro-metal dust generated from routine plant operations, directional dispersion of water vapor from the circulating cooling system, and the long-term accumulation of low-altitude, near-surface aerosols within the plant grounds. This creates a complex, high-intensity fog-induced optical interference field,This results in a faster rate of image quality degradation and a higher degree of distortion across the entire field of view. It is highly likely to trigger major high-risk operational safety hazards, such as blurred equipment outlines in monitoring images, failure of digital readings from on-site instrumentation, and the intelligent system's failure to detect dynamic targets intruding into high-risk perimeter zones, thereby severely limiting the all-weather, highly reliable, and stable closed-loop operation of comprehensive visual monitoring systems in nuclear engineering.Under foggy conditions across the entire area, high-density colloidal particles suspended in the atmosphere continuously intensify the effects of bidirectional scattering and directional absorption of incident light, directly causing common imaging defects such as a precipitous drop in dynamic contrast of captured images, irreversible loss of core operational feature information, and a general shift toward darkness in color and grayscale across the entire image.Such severe optical interference conditions have irreversible negative impacts on industrial-grade high-definition in-situ image and video acquisition chains. Consequently, the development of high-precision real-time image and video defogging technology—capable of adapting to all scenarios of specialized and demanding visual monitoring in nuclear engineering and addressing the shortcomings in front-end embedded in-situ

imaging quality—has become a critical, urgent, and cutting-edge research priority in the global nuclear industry's measurement and control sector.

Currently, mainstream lightweight image defogging algorithms worldwide are primarily implemented through software-based serial simulations using general-purpose high-level programming languages such as C++. While this purely software-based implementation approach has a low development threshold and manageable initial iteration costs, it suffers from poor cross-scenario portability and adaptability. Since the core computing chain employs a serial, data-by-data processing architecture, overall computational latency is relatively high,Their real-time processing capacity cannot meet the stringent requirements for millisecond-level synchronous closed-loop processing of high-definition video. This completely fails to satisfy the rigorous computational standards for nuclear engineering's comprehensive visual monitoring, which demands millisecond-level real-time imaging and 24/7 uninterrupted closed-loop surveillance. Consequently, these solutions struggle to meet the prerequisites for engineering deployment across all operating conditions, such as the local integration and deployment of compact embedded terminals within plant premises, as well as ultra-low-power, long-duration, unattended, and stable operation.Compared to traditional PC computing terminals, FPGA programmable logic chips offer core hardware advantages such as compact physical dimensions, ultra-low power consumption during full-range operation, excellent industrial-grade mobility, and maximum compatibility for on-board embedded integration. They can directly adapt to the harsh deployment conditions of nuclear engineering—including confined spaces within explosion-proof monitoring cabinets, strong electromagnetic interference, and fully sealed, dust-proof environments—enabling rapid installation, networking, and debugging.They are fully adaptable to various specialized monitoring scenarios in nuclear engineering, including dynamic monitoring of dedicated inspection corridors in nuclear facilities, fixed-point visual surveillance of reactor perimeter security, and round-the-clock visual closed-loop control of high-risk radioactive zones. This establishes a comprehensive, low-latency, real-time visual monitoring embedded computing hardware foundation for the entire

nuclear engineering chain.However, at this stage, general-purpose FPGA-based video defogging algorithms in the industry suffer from high computational complexity due to multi-dimensional iterative operations. These algorithms lack sufficient optimization for the complex optical conditions specific to nuclear engineering sites, where fog and dust often overlap. Achieving a balance among the three core requirements—ultra-low-latency defogging processing on the hardware side, full-range high-definition image fidelity, and long-term stable operation with strong anti-interference capabilities—remains a significant challenge requiring multi-dimensional optimization and breakthroughs.Accordingly, this paper addresses the critical safety production needs of comprehensive visual monitoring across all scenarios in nuclear engineering. It focuses on developing a lightweight, low-power, and highly efficient FPGA-based image and video joint defogging optimization algorithm tailored to the facility's multidimensional and demanding composite operating conditions.We have developed a comprehensive, integrated FPGA-based embedded video defogging system tailored for the nuclear industry—capable of immediate on-site deployment, featuring low power consumption and high stability, and delivering millisecond-level real-time response—thereby addressing the imaging and computing power gaps in high-end measurement and control scenarios within the nuclear sector.

1 Theoretical Foundations of Image Defogging Algorithms

1.1 Theoretical Foundations of Digital Image Processing

Digital images are primarily composed of two-dimensional structured pixel arrays. Leveraging standardized storage protocols, they enable comprehensive read/write control and real-time computing power allocation, and can be directly integrated with all types of industrial-grade embedded computing chips and dedicated digital circuits to perform real-time analysis and processing.The core pathway for comprehensive acquisition of high-definition digital images relies on dedicated optical imaging sensors to perform high-speed sampling of real-world optical signals. After precise quantitative closed-loop conversion, standardized digital pixel signals are generated. Comprehensive digital images can be categorized into two mainstream types: vector

high-definition images and raster bitmap images. The key differentiating factor is whether they possess the ability to adaptively adjust fixed grayscale contrast.In current industrial-grade visual monitoring scenarios, raster bitmap images serve as the core mainstream imaging medium. Standardized terms include "bitmap" and "pixel array," with a core architecture consisting of a two-dimensional structured pixel array arranged in fixed rows and columns. The intersection points of these rows and columns correspond to the smallest imaging unit—the pixel—which serves as the fundamental computational unit for global digital image processing. In single-channel grayscale images, a single pixel carries only the precise brightness quantification value corresponding to its coordinate position; In RGB color industrial monitoring images, a single pixel simultaneously integrates three-dimensional brightness characteristics and multi-dimensional color-layered dual-quantification information. Digital images can be directly captured and generated on-site using industrial-grade dedicated high-definition camera terminals, or they can be indirectly simulated and synthesized based on standardized digital calculation formulas, three-dimensional real-scene geometric simulation models, and other non-image-based structured data.Under equivalent computational load conditions, the computational logic of single-channel grayscale digital images is simpler and consumes fewer hardware resources. Each pixel carries only a single standardized grayscale sampling parameter, and the grayscale gradient can precisely cover the entire continuous range from pure black to pure white. Industry-standard two-dimensional continuous functions are used to achieve precise modeling and characterization of the entire grayscale image spectrum.In specialized scenarios for comprehensive visual monitoring of nuclear engineering, the system is equipped with 1080P or higher high-definition color raster imaging devices as standard across all sites to collect real-time, multi-dimensional operational footage of the facility around the clock. Pixel-level precision in brightness fidelity and native color reproduction directly determines the effectiveness of core, high-precision inspection tasks such as the automatic recognition of on-site instrumentation scales, the precise capture of micro-deformations on the outer walls of

large pressure vessels,and the assessment of latent hazards such as leaks in high-risk pipelines. This establishes a robust foundation of high-precision, standardized digital image processing capabilities and serves as a prerequisite for optimizing fog-reduction and enhancement performance in complex foggy conditions at nuclear engineering sites.

1.2 Resolution of Digital Images

The core quantitative definition of image resolution is: the total number of effective pixels that can be densely integrated and arranged within a display terminal per unit of physical dimension. Standardized quantitative labeling is achieved using the industry-standard two-dimensional pixel array format of width × height. Taking common industrial imaging parameters as an example, a resolution of 1024×768 represents an image with 1024 effective pixels arranged horizontally and 768 effective pixels arranged vertically.Currently, commercial and industrial-grade visualization terminals across all categories support a full range of mainstream resolutions, including 320×240, 640×480, 800×600, 1024×768, 1280×720 (720p HD), 1920×1080 (1080p Full HD), and 2560×1440 (2K Ultra HD), covering the full range of specifications;With the comprehensive iteration and upgrade of semiconductor storage chip technology and optical imaging sensor technology, 1080P Full HD imaging has become the universal, mainstream, standardized configuration for industrial vision monitoring scenarios worldwide, while 2K and 4K ultra-high-resolution imaging devices are gradually being adopted on a large scale.To address the dual critical requirements of long-term operation and maintenance, as well as low-power computing control in nuclear engineering's comprehensive visual monitoring environments, this study fully adapts to the mainstream standardized resolution of 1080P Full HD industrial-grade video capture terminals across the entire system.It simultaneously addresses three core requirements: optimal adaptation to the limited storage and computing power of onboard FPGA-based embedded systems; high-precision wide-angle imaging for long-distance, comprehensive panoramic inspections of nuclear facilities; and high-definition close-up imaging for on-site instrumentation. This approach effectively avoids the wasteful consumption of redundant computing power associated with ultra-

high resolution, as well as the safety hazards throughout the entire operational chain caused by misjudgments or missed detections resulting from the lack of critical operational details at lower resolutions.

1.3 Methods for Evaluating Image Quality

A quantitative image quality evaluation system is an indispensable core supporting technology for the field of global digital image processing. In the early stages, assessments of image quality were primarily based on subjective visual judgments, resulting in low evaluation efficiency and significant individual errors. This directly led to a substantial decline in the objectivity and reproducibility of evaluation results, rendering them unsuitable for industrial-grade, high-precision quantitative control standards.To address the shortcomings of subjective evaluation methods, the global scientific community has gradually developed a specialized technical framework for comprehensive, objective image quality evaluation that is standardized, quantifiable, and reproducible.The current industry-standard image quality assessment framework is uniformly divided into two core, parallel evaluation dimensions: human-based subjective tiered evaluation and machine-based objective quantitative evaluation. Among these, the objective quantitative evaluation system can be further categorized into three standardized technical paradigms based on the presence or absence of native fog-free reference images: full-reference quantitative evaluation, reduced-reference quantitative evaluation, and reference-free blind quantitative evaluation.In the comprehensive experimental evaluation phase of this study, we focused on four core computational dimensions—computational time for single-frame defogging, quantitative residual metrics for the entire image, entropy enrichment of effective image information, and average edge gradient clarity—to achieve a comprehensive, objective, and precise quantitative evaluation of post-defogging images.Concurrently, by benchmarking against globally accepted comprehensive safety control standards for nuclear engineering, the study rigorously verified three core compliance metrics in post-defogging monitoring footage: the integrity of critical electromechanical equipment edge contours, high-definition grayscale recognition of on-site

instrumentation, and ultra-low latency in real-time end-to-end transmission. This ensures that image quality evaluation results fully align with the entire closed-loop monitoring and refined operational maintenance standards required for nuclear engineering sites,This approach resolutely eliminates high-risk safety hazards arising from post-de-fogging algorithm optimization, such as color distortion in monitoring images, distortion of critical details, and excessive transmission latency.

1.4 Atmospheric Conditions on Foggy Days

1.4.1 Particles Under Different Weather Conditions and Their Effects

The core research scope of atmospheric optics focuses on the physical mechanisms underlying the full-path propagation of natural ambient light through the atmosphere, with an emphasis on fundamental optical processes such as refraction, directional reflection, and global scattering. Under severe fog conditions, high-density, large-radius colloidal particles suspended in the near-surface atmosphere—including industrial aerosol agglomerates,condensed water droplets from natural water vapor, interact with ambient incident light to produce intense coupled scattering, directional absorption, and secondary radiation effects. These significantly reduce the propagation efficiency of effective incident light, directly compromising the color fidelity, dynamic contrast, and quantitative metrics of multidimensional optical characteristics captured by visual imaging devices and the human eye during manual observation.Consequently, it can be concluded that the global light scattering effect of atmospheric suspended particles is the primary dominant cause of sudden drops in outdoor visibility and severe degradation of image quality in industrial applications, while other weakly correlated optical effects can be largely disregarded. Precisely dissecting the underlying physical mechanisms of image quality degradation in foggy conditions can effectively support the targeted iterative optimization of high-precision, directional defogging enhancement algorithms for images and videos under complex foggy conditions.This study specifically focuses on the unique enclosed atmospheric composite environment of nuclear power plant sites. It emphasizes an in-depth analysis of the dynamic evolution patterns of multidimensional light scattering interference resulting from the

dispersion of vapor and fine particles in unit circulating cooling water, the accumulation of metal dust from routine equipment operation and maintenance, and the superimposition and coupling of widespread natural fog. By precisely matching the complex on-site particle-optical conditions of the plant, the study optimizes and iterates the underlying optical adaptation logic of the defogging algorithm, comprehensively enhancing the front-end imaging system's overall resistance to optical interference in multi-gradient, complex fog scenarios within nuclear engineering facilities.

1.4.2 Model of Incident Light Attenuation

The coupling effect of high-intensity light scattering by atmospheric particulate matter is the fundamental underlying cause of irreversible degradation in the overall image quality of outdoor industrial imaging. Based on the conclusions of the atmospheric optics analysis discussed earlier, there is a strong correlation and coupling relationship between the physical radius of atmospheric particulate matter and the wavelength of incident light. When the equivalent radius of the particles matches the order of magnitude of the incident light wavelength, a global directional scattering model can be accurately established in a closed-loop manner.By leveraging the internationally recognized McCartney global atmospheric scattering standard illumination model, and integrating it with the incident light attenuation model and the global atmospheric imaging coupling model, it is possible to comprehensively and closed-loop decompose the entire chain of mechanisms leading to frame-by-frame image blurring and degradation under foggy conditions. The synergistic interaction of these two models directly induces severe degradation and deterioration of global image quality in outdoor environments.Specifically, the incident light attenuation model is primarily used to precisely quantify and decompose the underlying causes of frame-by-frame image quality degradation in foggy conditions. The core physical mechanism is as follows: effective incident light reflected from real-world monitoring points undergoes continuous scattering due to high-density suspended particles in the atmosphere, causing light energy to attenuate directionally along the transmission path in stages. The degree of attenuation exhibits a strict exponential positive correlation

with the physical observation distance.Within the closed-loop optical transmission system, a portion of the effective incident light undergoes multidirectional scattering, deviating from its original transmission path and failing to reach the visual observation and data acquisition terminal. This directly causes irreversible attenuation of incident light energy, with the attenuation magnitude increasing as the observation distance increases.Precisely tailored to the extensive, deep-reaching layout of nuclear power plant sites and the real-world operational conditions of long-distance, cross-unit, and cross-equipment closed-loop inspections, this system accurately calculates the quantitative coefficients of dynamic attenuation in long-distance optical paths.the model's core optical path compensation parameters are iteratively optimized to effectively mitigate the negative imaging interference caused by fog-induced light attenuation in long-distance, site-wide monitoring links, thereby comprehensively ensuring consistent grayscale and color uniformity across all monitoring images without blind spots.

1.4.3 Atmospheric Imaging Model

The global atmospheric light coupling model clearly indicates that the superimposed interference of global atmospheric light is another key contributing factor to the simultaneous degradation of image quality in industrial imaging under foggy conditions. The composite ambient light surrounding the equipment in real-world scenarios is formed by the coupling of three fundamental light sources: direct sunlight, global sky-scattered natural light, and ground-reflected ambient light. Each of these light sources possesses distinct optical spectra and brightness characteristics.Under foggy conditions with high particle concentrations, the ambient composite light is significantly disrupted by strong, directional reflections from suspended colloidal particles over a wide radius. Only a small proportion of effective light rays can travel along the intended observation path to the acquisition endpoint, directly affecting the quantitative indicators of effective light intensity received at the observation end. Due to the comprehensive influence of this mechanism, industrial images captured in situ under foggy conditions typically exhibit characteristic defects such as overall grayish-

white tones and blurred details.Direct natural sunlight, ground-level scattered light, and global atmospheric scattered light are collectively defined as the global composite atmospheric light spectrum. Considering the specific on-site environment characterized by the dense arrangement of enclosed structures in nuclear engineering facilities, uneven natural lighting in localized areas, and the routine use of global artificial auxiliary lighting,we have specifically optimized the core logic of adaptive compensation for global atmospheric light balance. This effectively mitigates issues such as global image whitening and monitoring blind spots in dark areas caused by the overlapping interference of local direct strong light, weak light blind spots, and foggy conditions, thereby comprehensively adapting to the complex, site-specific lighting conditions across all monitoring locations within the facility.

2. Algorithm Research

2.1 Histogram Equalization Algorithm

Let the probability density function of the image be denoted by (p(x)), the probability density function of the original image by (pr(r)), and the probability density function of the grayscale-mapped image by (ps(s)). Then we have:

$$Ps\ （s）= \mathrm{pr}\ （\mathrm{r}）\ \frac{\mathrm{d}r}{\mathrm{d}s}$$

$$s = f(r) = \int_o^r pr(u)du$$

From the two formulas above, we can see that for grayscale values in the range [0, 255], when multiplied by the corresponding maximum grayscale value Dmax, the mapping formula for histogram equalization becomes:

$$DB = f(DA) = Dmax \int_o^{Da} PDA(u)du$$

Here, DA represents the grayscale values of the original image, and DB represents the grayscale values after grayscale mapping.

Next, apply the above equation to discrete variables:

$$DB = \mathrm{f}(\mathrm{DA}) = \frac{Dmax}{\mathrm{Ao}\sum_{imn}^{DA} N(i)}$$

In the formula: N(i) represents the total number of valid pixels in the global image at grayscale level i, and A0 represents the total number of valid pixels in a single frame of high-definition image.During the initial debugging and adaptation phase of the algorithm, it targets the multi-gradient, differentiated grayscale imaging characteristics of on-site nuclear engineering equipment—including dark-colored metal pressure vessels, light-colored specialized safety protective coatings, and high-brightness local instrument dials—to finely tune the critical thresholds for global histogram equalization and adaptive grayscale mapping.This approach simultaneously addresses the dual core objectives of efficiently enhancing overall imaging contrast while fully preserving critical local operational details of the equipment, precisely meeting the essential requirement for high-definition grayscale imaging in the refined closed-loop inspection of nuclear facility units.

2.2 Histogram Stretching Algorithm and Implementation Steps

The classic global histogram equalization algorithm has inherent technical limitations; high-intensity equalization iterations can easily lead to irreversible loss of critical operational details in local image regions, as well as blurring and distortion of edge contours, making it unsuitable for the high-precision inspection imaging standards required in nuclear engineering.In the full processing chain for high-precision industrial real-world image processing, the adaptive histogram stretching optimization algorithm is prioritized. Leveraging the computational logic of directional grayscale linear mapping, this algorithm adaptively stretches the grayscale parameters of pixels within locally constrained ranges to fully cover the standard grayscale range of 0–255.Raw images captured from real-world scenes are commonly overlaid with random dust noise and electromagnetic pulse interference. It is necessary to optimize the core adaptation parameters of the algorithm based on specific on-site conditions. The global standardized computational formula is as follows:

$$f(x,y) = \frac{255}{\mathrm{M} - N}(f(x,y) - N)$$

Here, M and N represent the maximum and minimum values of the input image's

grayscale, respectively, while f(x, y) and f'(x, y) represent the pixel grayscale values before and after stretching, respectively. Here, we assume that the image is stretched to the range [0, 255]. Based on the above equation, the FPGA implementation of the histogram stretching algorithm is as follows:

Determine the upper and lower thresholds, Thr_max and Thr_min, based on the input image; calculate the coefficients M and N;

Calculate the difference between each pixel and N;

Calculate the value of 255 / (M - N);

Multiply the results obtained from (3) and (4). To address the challenges of narrow grayscale dynamic range and blurred grayscale gradients along equipment edges in nuclear engineering foggy images, we have optimized the adaptive threshold matching mechanism for histogram stretching. This enhances grayscale layering in critical areas such as equipment outlines, pipeline interfaces, and security fences within the plant, precisely meeting the essential requirements for detailed monitoring of high-risk locations in nuclear engineering.

2.3 Fog Removal Algorithm Based on Dark Channel Prior Reconstruction

This algorithm is based on statistical patterns identified after analyzing a large number of outdoor images. Specifically, in most outdoor images, the intensity of pixel values in certain areas of at least one color channel (R, G, or B) is extremely low, approaching zero. By leveraging this pattern, the algorithm can directly estimate the thickness of fog in the image and then restore the image to a high-quality, fog-free version.

For an image J, the dark channel can be expressed mathematically as:

$$Jdank(x) = \min(\min(Jc(y)))$$

Here, `Jc(y)` denotes the color channel of image `J` (i.e., one of the three channels: R, G, or B), `(x)` denotes a local window centered at `x`, and `Jdark` denotes the dark primary color of image `J`. According to the theory of prior-based dark primary color recovery and the definition of the dark channel, for a fog-free image `J`, the value of `Jdark` in the formula tends to zero.

The relationship between image information and image transmittance is as follows:

$$I(x) = J(x)t(x) + A(I - t(x))$$

(X) represents the hazy image within a local window centered at X; t(X) represents the transmittance of the local window centered at X; and a is the atmospheric light value, calculated as the average of the top 0.1% of pixels in the dark primary image within the local window.Divide both sides of Equation (7) by Ac (where c is one of the R, G, or B channels), and then perform two rounds of minimum filtering on both sides of the equation. Substituting the results into the equation yields the following:

$$J(x) = \frac{\mathrm{I}(x) - A}{\max(t(x)t0} + A$$

Here, t0 represents the minimum threshold value for image transmittance, I(x) denotes the foggy image, and A denotes the mean of the top 0.1% of pixels by brightness in the dark reference image. The core algorithm optimization in this paper is deeply tailored to the demanding real-world conditions of visual monitoring in nuclear engineering. It focuses on iteratively optimizing the core computational strategy of adaptive windowing and weighted filtering in the dark channel, precisely correcting inherent algorithmic defects that cause high-luminance halos in bright metal structures and areas with concentrated artificial lighting within the plant. Simultaneously, the algorithm is enhanced to resist plant dust noise andelectromagnetic pulse interference. It simultaneously addresses the dual objectives of high-precision defogging image quality and millisecond-level real-time parallel computing performance under complex, mixed fog and dust conditions, fully meeting the industrial-grade operational compliance standards for 24/7 uninterrupted visual monitoring in nuclear engineering.

3. Experimental Testing Platform

The core control chip selected for the All-Domain Experiment is the industrial-grade Altera Cyclone IV series FPGA chip EP4CE6E22C8. This chip features abundant and redundant native logic hardware resources, with a rated maximum stable operating clock frequency of up to 472.5 MHz.This self-developed integrated real-time embedded defogging system for all-domain video, following full-process synthesis, compilation,

and closed-loop verification of layout and routing via EDA tools, exhibits an internal effective logic hardware resource utilization rate of less than 75%. The hardware layout and routing are orderly and reasonable, with no redundant losses in the computing chain.This industrial-grade FPGA chip offers three core hardware advantages: ultra-low rated operating power consumption, strong all-area electromagnetic interference resistance, and compact on-board integration. It is perfectly suited for specialized monitoring cabinets in nuclear engineering facilities with sealed electromagnetic shielding,outdoor explosion-proof and dust-proof standalone monitoring terminals, fully meeting the unified standards for long-term industrial-grade hardware operation and maintenance management within plant facilities. It requires no additional hardware modifications for adaptation and can be directly integrated into existing nuclear engineering comprehensive visual monitoring networks at nearby locations, enabling rapid large-scale deployment and networking.

A full-frame front-end video and image data acquisition module, featuring the industrial-grade CMOS image sensor OV7725 as standard equipment, equipped with a dedicated I2C high-speed serial bus interface. The industrial-grade CMOS image sensor highly integrates photoconversion and signal preprocessing units, achieving a native maximum HD video capture and transmission frame rate of 30 frames per second. It incorporates a high-speed A/D converter, a front-end DSP image preprocessing unit, and a standardized I2C bus control unit, providing a full-chain computing capability.The sensor’s native image sensor array has a total pixel resolution of 656 × 488; in real-world engineering tests, the effective imaging resolution is 640 × 480. It supports multiple mainstream industrial HD video and image data output formats and is compatible with comprehensive computing power integration and debugging. The I2C high-speed serial bus integrates a serial clock (SCL) andand serial data (SDA) to form a dual-channel core transmission link. Within the full spectrum of industrial communication bus systems, it offers core advantages including excellent serial communication speeds, stable 8-bit bidirectional data exchange, and simplified yet versatile external interface adaptability. In low-power serial mode, the stable

transmission rate reaches 100 Kbit/s, with a maximum peak transmission rate of 3.4 Mbit/s.The accompanying camera acquisition modules fully meet industrial-grade standards for dust and water resistance, as well as stringent requirements for wide temperature ranges and resistance to deformation. They can be directly deployed in high-dust outdoor inspection areas for nuclear engineering projects and in complex indoor scenarios such as enclosed maintenance compartments for equipment units. The bus data transmission remains stable throughout the process and is resistant to electromagnetic interference, effectively preventing video frame loss,stuttering, and link interruptions caused by complex electromagnetic conditions within the plant, ensuring comprehensive, continuous, and uninterrupted closed-loop visual monitoring operations.

The in-house developed FPGA controller development board comes standard with a dual-core storage unit comprising a 64M high-speed SDRAM synchronous dynamic cache chip and an M25P16 high-capacity solid-state storage chip.High-speed SDRAM offers core advantages such as fast instantaneous data read/write speeds, high functional density per unit area, and strong adaptability for parallel computing power scheduling. It utilizes an industrial-grade high-speed CMOS architecture dynamic random-access memory (DRAM) medium, with programmable burst transfer lengths that are dynamically adaptive and adjustable, comprehensively meeting the requirements for multi-link concurrent computing power scheduling.Ample onboard high-speed cache resources efficiently support real-time scheduling of concurrent defogging computing power for synchronized, cyclical video monitoring across multiple units and locations in nuclear engineering.Large-capacity solid-state storage units enable short-term closed-loop retention of both composite fog-state raw monitoring footage and algorithm-optimized high-definition standard images, facilitating subsequent long-term operational traceability and review for nuclear engineering, as well as the digital archiving and closed-loop management of operational logs under all conditions. This fully aligns with the core requirements for standardized, traceable control throughout the entire process of global nuclear industrial safety production.

4. Experimental Design and Analysis

4.1 An FPGA-Based Dehazing Algorithm Platform

The overall system block diagram is shown in Figure 1.

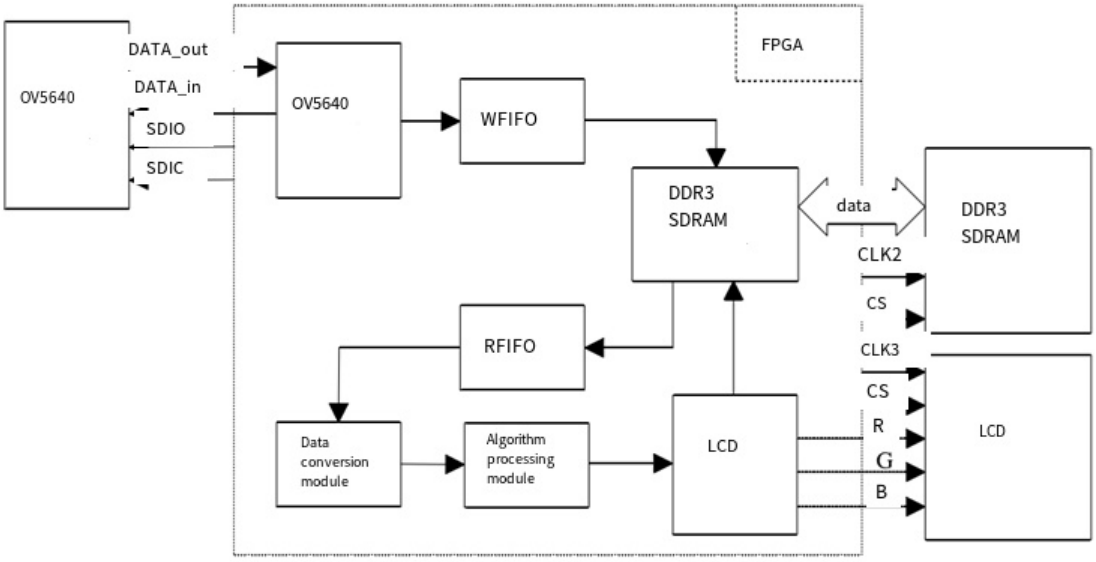

Figure 1: System Flowchart

The overall hardware logic architecture and closed-loop computing workflow of the in-house developed system are shown in Figure 1. In this integrated embedded image processing computing platform, the FPGA core chip serves a dual-core function, acting as both the central hub for global instruction coordination and the core hub for parallel, high-speed real-time data processing.Under the precise control of the FPGA's timing logic instructions, the front-end high-definition image acquisition submodule captures raw, real-time, all-weather video data of the plant site in situ. This data is uniformly packaged into a standard RGB pixel data format for directed output and is synchronously transmitted via a closed-loop to the onboard high-speed image cache storage submodule for temporary caching.Under the precise coordination of global timing control signals, the in-house optimized defogging algorithm processing submodule rapidly reads the raw image pixel data from the cache to perform end-to-end, directional defogging with enhanced parallel computing power. Finally, the standardized data of the high-definition, defogged images is directed to the terminal visualization display submodule, which uses an industrial-grade high-definition LCD screen to output the real-time, closed-loop restored global monitoring video feed.As

shown in Figure 1, the overall architecture divides the entire computing system into three core interconnected units: the front-end CMOS camera high-speed data reception unit, the global image and video big data cache scheduling unit, and the back-end algorithm parallel computing and visualization output unit.The raw data from pre-processed real-time video is cached in a closed-loop system within DDR3 high-speed SDRAM to enable precise time-division multiplexing control over read/write operations. The high-definition, fog-free video, optimized by algorithms, is displayed in real time via a standardized VGA driver interaction module.The entire computing platform adopts a minimalist, modular, and layered architectural design, enabling seamless integration with mainstream commercial vision monitoring and control integrated platforms used in nuclear engineering sites worldwide. There is no need to reconfigure existing global networking and transmission links; the system supports plug-and-play rapid deployment, precisely addressing the core engineering requirements of nuclear engineering sites: rapid deployment, low operational and maintenance overhead, and high hardware compatibility.

4.2 Modules of the Video Defogging System

4.2.1 Image Acquisition Module

This in-house developed FPGA-specific development board features an integrated 18-pin industrial-grade HD CMOS standardized camera expansion interface, enabling seamless compatibility with the OV5640 HD industrial camera module to quickly establish a closed-loop system for real-time, all-weather, in-situ HD video capture.After capturing the entire scene, the system supports flexible dual-mode image visualization: local real-time playback on an industrial-grade TFT LCD screen or external connection to a professional control room monitor via a standardized high-speed VGA interface. The integrated OV5640 camera sensor unit combines the dual core advantages of high-performance HD imaging and ultra-low power consumption, making it perfectly suited for long-term, unattended embedded operations. The OV5640 module exhibits a strict inverse relationship between video resolution and real-time output frame rate: as imaging resolution increases, the effective transmission frame rate decreases

proportionally, with the product of the two remaining constant and equal to the link's rated transmission bandwidth limit.As shown in Figure 2, this is the RTL logic timing diagram for the global functional simulation of the front-end image acquisition module. The module is hierarchically decomposed into three interconnected subunits: the dedicated register timing configuration control subunit `reg_gen`, the 8-to-16-bit high-speed parallel data transmission subunit `cmos_8_16bit`, and the global phase-locked loop clock synchronization control subunit `video_pll`.The reg_gen subunit globally incorporates a complete set of standardized configuration parameters for the OV5640 camera module's dedicated control registers, while the cmos_8_16bit subunit precisely adapts to the camera module's global timing interaction logic, ensuring lossless, high-speed transmission of captured data.

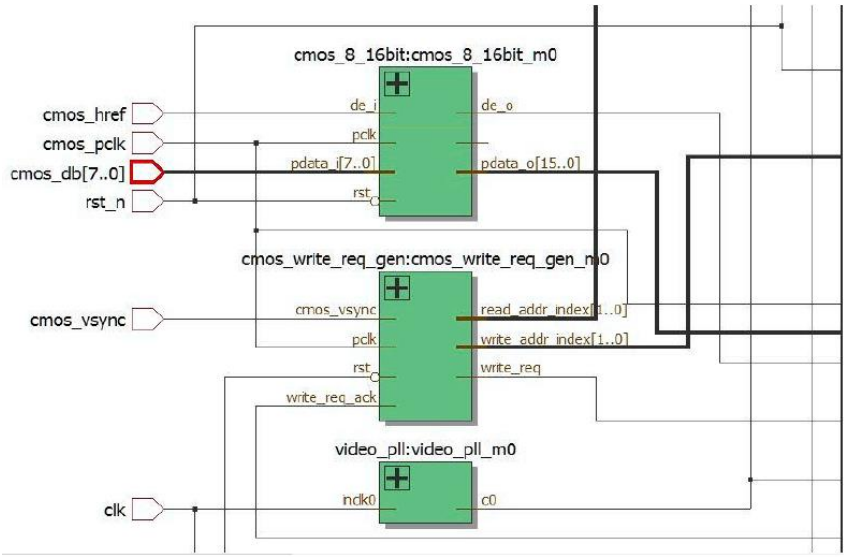

Figure 2: RTL View of the Image Acquisition Module

4.2.2 Image Storage Module

The in-house development board features a single industrial-grade dedicated SDRAM cache chip, specifically designated as the HY57V2562GTR, with a rated storage capacity of 256 Mbit and a standardized 16-bit parallel high-speed data bus.The primary function of this SDRAM is to serve as a high-speed data relay cache for real-time, full-domain images, enabling the temporary storage of raw video data captured in situ, time-division multiplexing of read/write operations for algorithmic processing, and closed-loop empowerment of cross-module data interaction throughout the entire

process. Ultimately, it integrates with a VGA visualization terminal to enable high-definition image output and playback.This system fully supports SDRAM with a rated physical storage capacity of 256 Mbits, internally divided into 4 independent parallel high-speed storage units, each with an independent rated storage capacity of 4 Mbits.Equipped with a dedicated multi-channel parallel dual-port RAM computing architecture, the system leverages a specialized ping-pong cache mechanism for time-division read/write parallel operations to efficiently resolve the technical challenges of image frame trailing and picture discontinuity—common issues in the high-definition fog-removal computing chain.It achieves global asynchronous parallel time-division read/write operations and seamless, rapid switching between multiple storage units, maximizing the utilization of hardware parallel computing resources to establish a high-speed, continuous pipeline-style closed-loop image processing architecture.It prioritizes the high-speed writing of raw video data captured in situ by the front end to independent storage unit 0, while simultaneously scheduling the algorithm processing module to retrieve cached data from storage unit 3 to perform parallel defogging operations, ensuring that data writing and computational processing advance in a bidirectional, asynchronous yet synchronized manner;Once the full-frame image data has been written into the closed-loop system, the system automatically and seamlessly switches to read from and write to the corresponding independent storage unit, repeating this cycle to achieve round-the-clock, uninterrupted parallel computing resource scheduling.This architecture not only efficiently addresses the inherent limitation of limited storage resources in embedded onboard hardware but also comprehensively enhances the instantaneous computing power for single-frame image processing, fundamentally eliminating high-frequency frame-to-frame trailing and image stuttering defects in industrial surveillance video at the hardware level.The dedicated hardware architecture for global parallel read/write "ping-pong" caching fully addresses the critical need for 24/7 uninterrupted closed-loop continuous monitoring and imaging in nuclear engineering,It guarantees no image stuttering, no loss of valid frames, and no trailing or ghosting effects throughout the entire process,

establishing a robust computational foundation for seamless and complete monitoring of all critical points within high-risk nuclear facilities. This eliminates the risk of operational misjudgments caused by image discontinuities or distortions.

4.2.3 Video Transmission and Display Module

Since the era of classic CRT displays, the VGA (Video Graphics Array) standardized video interface has long been widely adopted across all industrial visualization and control scenarios due to its stable transmission, broad adaptability, and strong compatibility. The VGA interface standard, also known as the D-Sub interface, features a proprietary D-shaped physical connector with 15 standardized pins arranged in three evenly spaced rows, with five pins per row.The core functional pins include three pins for transmitting analog RGB color signals, as well as two dedicated pins for scan timing synchronization: horizontal sync (HSYNC) and vertical sync (VSYNC). The RGB signal source terminals are equipped with standardized 75-ohm termination resistors to ensure signal transmission without attenuation or distortion. The architecture of the standardized VGA video signal transmission chain is shown in Figure 3.

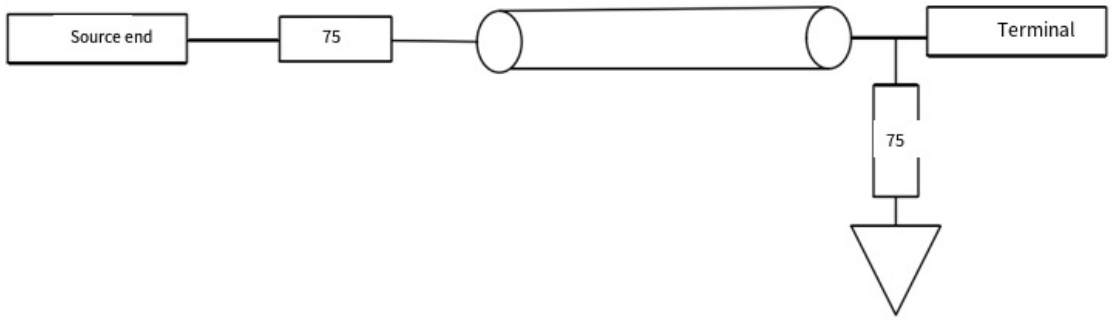

Figure 3: Schematic Diagram of VGA Video Signal Transmission

Both the HSYNC horizontal synchronization signal and the VSYNC vertical synchronization signal are compatible with standard TTL logic levels. The FPGA core chip can only output native digital logic signals, whereas the VGA interface requires three-channel RGB analog video signals. By utilizing a simple, high-precision resistive voltage divider circuit, it achieves lossless closed-loop conversion from digital to analog signals, enabling stable output of 32-level gradient red and blue primary color signals and 64-level high-precision gradient green primary color signals, maximizing

color reproduction fidelity.Through fine-tuned dynamic adjustment of resistor values, the system flexibly adapts to overall signal strength and enables real-time adaptive brightness control of the display.Following a modular, layered design logic for the entire system, the process sequentially completes the writing of hardware logic code, comprehensive simulation of the entire system logic, closed-loop verification of timing functions, and on-board hardware testing, ultimately achieving the full-scale deployment of an integrated defogging vision system and precisely meeting the preset experimental technical specifications. The RTL timing simulation logic view of the backend high-definition image visualization output module is shown in Figure 4.

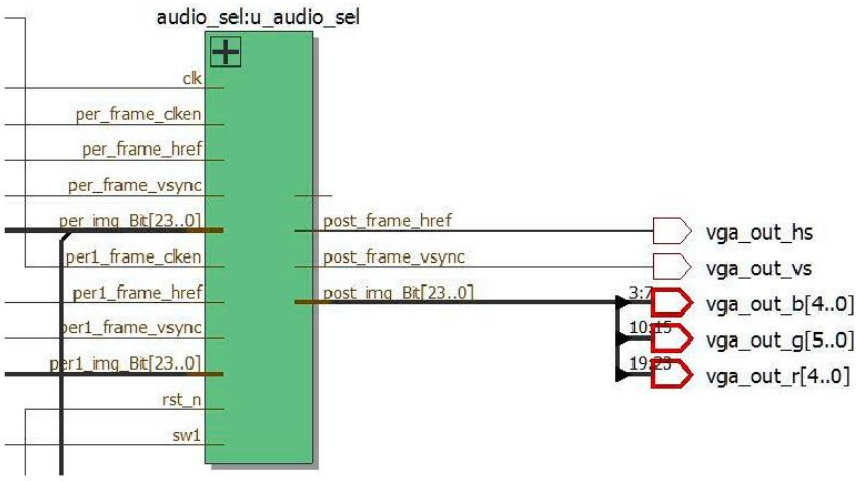

Figure 4: RTL View of the Image Output Module

4.3 FPGA Implementation of the Dark-Channel Prior Algorithm

By integrating the computational logic for high-precision defogging of single static images with the native parallel processing capabilities of FPGA embedded chips, and by adopting a proprietary modular, layered, and decoupled parallel acceleration design philosophy across the entire system, we have successfully adapted, ported, and optimized the algorithm for the hardware platform.By anchoring on the fundamental features of fog-degraded real-world images, we decompose the standardized fog-removal computational workflow into a closed-loop process across the entire chain. This involves sequentially performing parallel computation of dark-channel feature maps, precise estimation of global atmospheric optical equivalents, real-time adaptive correction of transmittance, and closed-loop parallel modeling for the reconstruction of

high-definition fog-free images. This approach maximizes the utilization of hardware parallel computing capabilities, exponentially increasing the real-time processing speed of the global algorithm.By analyzing the core characteristics of continuous imaging in dynamic video, we determine that there are no significant abrupt changes in the background scene structure or optical environmental parameters between adjacent video frames. This enables effective suppression of high-frequency brightness flickering andand color jumps caused by operational interference. The core computational parameters for atmospheric light and transmittance, derived from high-precision calculations of preceding reference frames, are reused and adapted to the closed-loop image restoration computational chain for the current video frame under processing. This significantly reduces redundant computational overhead while simultaneously optimizing the visual comfort of the dynamic video across the entire scene.By leveraging the pre-set critical thresholds to precisely calculate global atmospheric light equivalent quantification parameters, the system time-shares the use of signals processed from preceding frames within the SDRAM cache. This triggers the directed output of raw foggy image data for the next frame, enabling frame-by-frame closed-loop scheduling of the entire high-definition image restoration process.Utilizing a pipelined parallel computing architecture, we comprehensively reduce the end-to-end processing latency for single-frame image defogging. This ensures stable compliance with the stringent technical requirements for millisecond-level real-time transmission in nuclear engineering visual monitoring. The system delivers a seamless viewing experience throughout—free of screen flicker, color shifts, or detail distortion—ensuring a comfortable viewing experience for operations personnel during prolonged, routine monitoring in control room duty stations.

The global algorithm is decoupled into four independent parallel computing submodules: the high-speed dark-channel feature map computation submodule, the global atmospheric light equivalent value synchronous estimation submodule, the real-time transmittance adaptive correction submodule, and the high-definition image closed-loop restoration output submodule. A multi-unit collaborative parallel

computing architecture is established for the global algorithm, and the complete computing scheduling process is shown in Figure 5.Raw pixel data from global real-time video is output at high speed in a standardized 24-bit RGB data stream format via the front-end acquisition module and simultaneously cached in the onboard SDRAM high-speed storage unit;Simultaneously retrieves global pixel data from the preceding reference frame, employs a 5×5 adaptive weighted sliding computation window, and rapidly completes the parallel computation of global dark channel feature maps; synchronously coordinates parallel computation links to perform closed-loop calculations of global atmospheric light equivalent quantification parameters and real-time per-pixel transmittance parameters for each frame;Finally, the system couples the raw data from the current frame's native fog-degraded image with core restoration formulas to complete a closed-loop reverse calculation, accurately outputting high-definition, lossless, fog-free monitoring images. Leveraging a modular parallel computing architecture, the system exponentially enhances the real-time processing efficiency of the algorithm across the entire system, balancing the dual core metrics of high-precision defogging image quality and ultra-low latency computing performance.

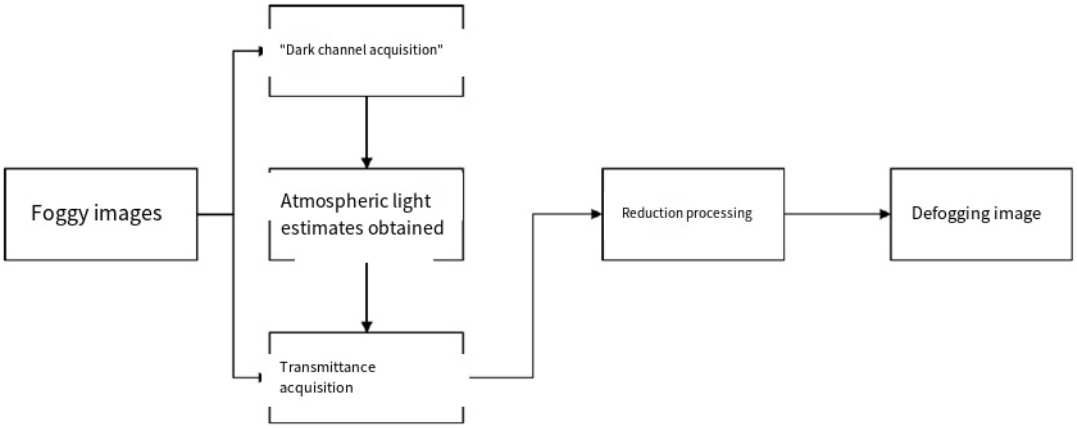

Figure 5: Flowchart of the video defogging algorithm

4.3.1 Determining the Minimum Dark Channel

Due to the computational power limitations of industrial-grade video codec chips and the hardware constraints associated with implementing lightweight embedded algorithms, the input video resolution is standardized across the entire system.The 1080p industrial-grade HD video standard was selected, featuring 1,125 horizontal

precision scan lines and 1,080 effective visible horizontal scan lines. The native resolution is locked at 1,920 × 1,080, and the system achieves a stable operating frame rate of 60 fps in all scenarios.The algorithm synchronizes with a three-channel RGB collaborative computing architecture. Input video is uniformly standardized to a 24-bit full-color-gamut, lossless HD RGB format, with the R, G, and B primary color channels uniformly covering the full 0–256 brightness quantization gradient. This enables the reconstruction of 16.78 million real-world colors across the entire spectrum, fully meeting the critical requirement for color fidelity in industrial imaging.By imposing dual constraints on standardized resolution and color gamut formats at the front end, the system ensures comprehensive compatibility and stable operation of the algorithm across different hardware and operating conditions. It perfectly aligns with the mainstream specifications of front-end camera equipment used for global nuclear engineering visual monitoring, enabling seamless integration of computing power without the need to replace existing front-end hardware. This significantly reduces the overall cost of implementing intelligent upgrades at nuclear engineering sites.

Traditional dark channel prior algorithms are prone to artifacts such as luminance halo distortion in high-brightness outdoor sky areas and areas with intense artificial lighting. To address this, the core logic for dark channel estimation has been optimized and iterated to leverage the parallel computing capabilities of FPGA hardware. In the global defogging algorithm, multi-stage filtering across the entire processing chain serves as the core foundational unit, and the accuracy of the dark channel estimation process directly determines the final image quality of the defogged output.In the software simulation platform, images are stored globally as complete two-dimensional pixel matrices, allowing for the free retrieval of pixels at any coordinate to perform window filtering operations, with no mandatory constraints on pixel retrieval timing. However, since the FPGA hardware operates based on a pipelined parallel data flow architecture, the filtering timing logic must be specifically restructured, and the computational chain must be optimized for efficiency.

As shown in Figure 6, the lightweight dark-channel parallel solution architecture

developed in this paper consists of two levels of interconnected computing units: In the first level, the R, G, and B primary color channels of a single frame are compared pixel-by-pixel in real time to quickly extract the global minimum grayscale value for each channel, thereby generating an initial grayscale feature map;In the second stage, a lightweight recursive filtering architecture is employed, utilizing two-stage 3×3 small-sized sliding window recursive iterative filtering. This effectively achieves the computational performance equivalent to a 5×5 large-window global minimum filtering operation, rapidly generating a standard dark channel feature map with high precision.This optimized lightweight recursive computing solution significantly reduces FPGA hardware logic resource consumption and lowers real-time power consumption while maintaining zero-loss, high-definition defogging image quality. It is perfectly suited for long-term, unattended, stable operation on low-power embedded edge devices in nuclear engineering applications and fully complies with industrial-grade on-site computing low-carbon control and access standards.

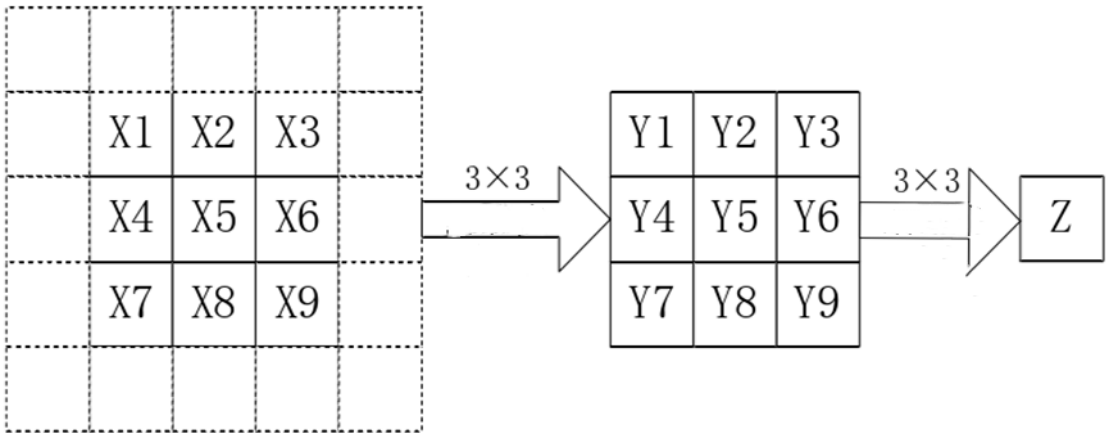

Figure 6: Dark-channel subtraction process

4.3.2 Estimation of Atmospheric Light Value

By reusing the closed-loop computational formula for the standardized atmospheric light value A described earlier, we have specifically adapted and packaged the logic for the FPGA hardware side and integrated a dedicated hardware computational submodule. After completing the high-speed closed-loop solution for the dark channel feature map, we invoke the FPGA's built-in Shift Register IP core to generate multiple synchronized parallel computational data links, thereby enhancing

computational real-time performance.Leveraging the core characteristic of weak fluctuations in real-world optical parameters between adjacent video frames, the system uses the high-precision atmospheric light quantification value calculated for the current frame as the initial reference value for the next frame. This significantly reduces redundant computational overhead associated with frame-by-frame processing and exponentially improves the real-time frame rate for global video processing.By synchronously overlaying and smoothly interpolating quantified atmospheric light values between frames, the system effectively mitigates high-frequency flickering defects caused by abrupt changes in atmospheric light parameters between adjacent video frames. This approach adapts to complex real-world conditions in nuclear power plant facilities, such as the alternating activation and deactivation of natural daylight and the dynamic switching of localized artificial lighting. It ensures a stable and comfortable visual experience throughout the monitoring process without compromising the precision of identifying and quantifying minute equipment malfunctions.

4.3.3 Determination of Transmittance

By integrating the optimization methods described earlier to determine global dark-channel characteristic quantization parameters and adaptive atmospheric light equivalent quantization parameters, and by substituting these into the standardized transmittance computation formula in a closed-loop process, the system performs high-speed, pixel-by-pixel parallel computation to determine real-time dynamic atmospheric transmittance quantization metrics. The global computation logic is fully consistent with the software simulation algorithm benchmarks described earlier.Figure 7 shows the simulation output waveform of the real-time transmittance high-speed solution on the hardware side. The waveform is smooth and distortion-free, and the computational response is latency-free, meeting the real-time computational performance specifications for embedded hardware.

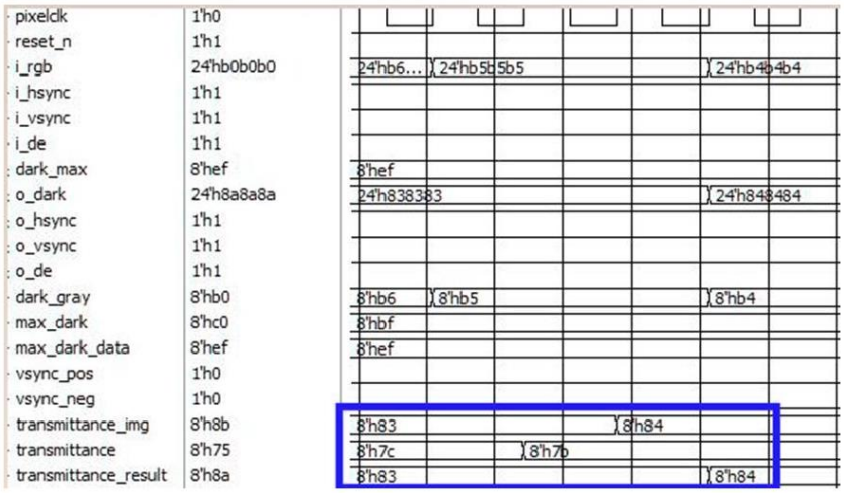

Figure 7: Simulation diagram for determining transmittance

4.3.4 Fog Image Restoration

The Image Precision Restoration Module serves as the core output unit at the end of the global defogging algorithm. It processes four parallel input parameters: globally optimized dark channel feature maps, real-time dynamic transmission parameters at the pixel level, globally adaptive atmospheric light equivalent constant parameters, and raw data from in-situ captured images showing fog degradation. By integrating these parameters with standardized closed-loop restoration formulas, the module performs reverse calculations to accurately output high-definition, fog-free standard real-world images.To avoid calculation errors caused by transmission values approaching zero, a global safety threshold of 0.2 is preset as the lower limit.To address the inherent limitation of FPGA hardware in performing high-speed floating-point operations, a fixed-point optimization and adaptation have been implemented: the global threshold is amplified by a factor of 255 to facilitate integer conversion, while all other global parameters are shifted left by 8 bits, effectively amplifying them by a factor of 256.The hardware arithmetic logic for integer operations was simplified throughout the process, resulting in negligible computational loss and no degradation in image fidelity.The hardware simulation results are shown in Figure 8. Compared to the native RGB quantization parameters obtained from the dark channel solution simulation, the pixel brightness and color quantization parameters across all three channels of the image are significantly optimized and enhanced after defogging. Image details are fully restored,

thoroughly validating that the algorithm, when ported to FPGA hardware, delivers excellent defogging performance and exceptional hardware adaptability, making it suitable for large-scale engineering implementation.

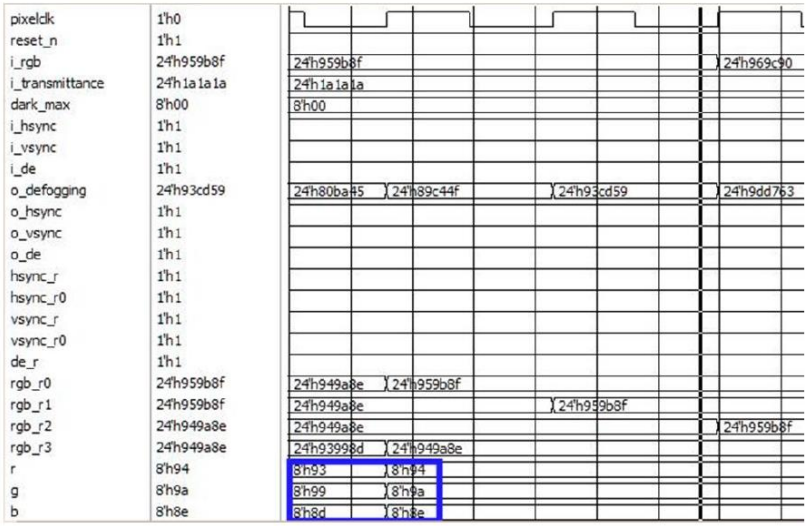

Figure 8: Simulation of a defogged image

5. Experimental Results and Resource Utilization

5.1 Experimental Results

We established realistic simulation environments replicating typical nuclear engineering conditions, including multi-gradient composite fog and dust, low-temperature high-humidity, and strong electromagnetic interference. We completed end-to-end closed-loop comparative testing of onboard hardware, and the results of these comprehensive comparative experiments are shown in Figure 9.The left column of each image set consists of raw monitoring images capturing the degradation of native fog conditions collected on-site at the facility, while the right column shows high-definition, fog-free restored images processed in real time via parallel processing using optimized algorithms on the FPGA hardware. The first two sets of comparison samples demonstrate the fog removal results for static real-world images, while the latter two sets demonstrate the closed-loop fog removal results for dynamic real-time surveillance video frames.The comprehensive real-world test results fully validate that the self-developed embedded integrated FPGA defogging system can stably perform millisecond-level high-precision closed-loop defogging and enhancement processing on high-definition images and real-time video around the clock, operating without lag,

crashes, or image distortion.From the perspective of subjective visual assessment, after strictly controlling for interference errors caused by stray light reflections in the experimental environment, the images were processed using our proprietary optimized algorithms. This resulted in a significant improvement in the restoration of native colors, the integrity of edge details, and overall image clarity, demonstrating excellent comprehensive defogging performance.From the perspective of real-time computational efficiency, the system maintains a stable frame rate of 60 fps across the entire monitoring area during live video testing. This fully meets the real-time display frame rate standards for industrial-grade HD video, with millisecond-level closed-loop processing, precisely achieving the core technical objectives of all-weather real-time defogging.Specialized closed-loop comparative tests were conducted across the entire facility to simulate multiple high-risk operational scenarios typical of nuclear engineering sites, including complex fog-dust coupling, low-temperature high-humidity condensation, and aerosol accumulation in enclosed spaces. Following defogging optimization, critical fine-detail monitoring features—such as the external pressure pipelines of nuclear facilities, the closed-loop security fencing across the entire site, the on-site high-precision instrument scales, and minute deformation traces on equipment—were fully and clearly restored. The results are free of halo artifacts, detail distortion or loss, and color shifts or distortions, fully meeting global standards for the quantitative accuracy and compliance of visual inspection and verification in nuclear engineering safety production.

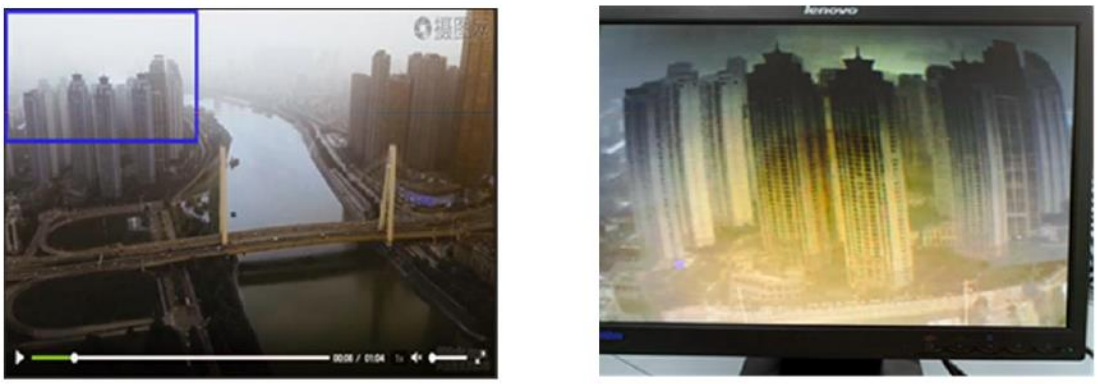

Figure 9: Experimental results of the video defogging system

A comprehensive comparison of the actual footage reveals that the original image on the left is uniformly blurred and hazy, with the outlines of distant equipment obscured by fog and dust; After fog removal via FPGA hardware-based algorithm optimization, the high-definition image on the right clearly reveals the contours and textures of factory buildings shrouded in light fog at a distance, while the colors of nearby equipment and vegetation are naturally restored with uniform brightness. The overall visual observation experience has been significantly enhanced.Field tests confirm a stable operating frame rate of 60 fps. Image capture, parallel algorithmic processing, and real-time video output proceed asynchronously across the entire chain, achieving ultra-low latency at the millisecond level. This fully meets the mandatory latency standards for real-time transmission in nuclear engineering central control monitoring systems, enabling seamless integration into existing integrated security monitoring platforms for routine, large-scale deployment.

5.2 Resource Utilization

The real-time statistics on the overall hardware resource utilization of the in-house developed integrated defogging system are shown in Figure 10 and Table 1. Key statistical metrics cover comprehensive hardware parameters, including logic units, timing registers, on-board memory bit resources, and virtual pin resources. Overall resource utilization is reasonable and controllable, with ample redundant resources. The system offers a low overall hardware implementation cost and is suitable for large-scale, batch network deployment.

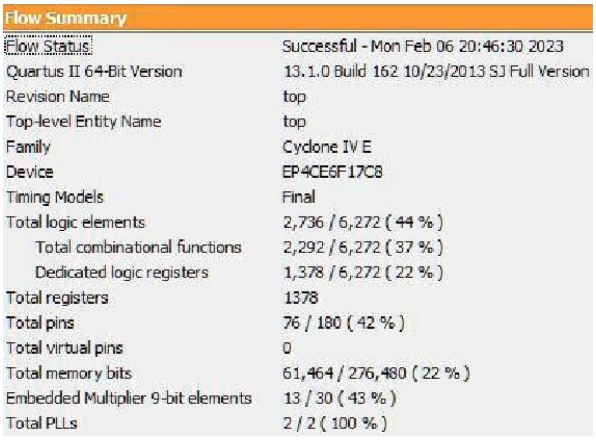

Flow Summary	
Flow Status	Successful - Mon Feb 06 20:46:30 2023
Quartus II 64-Bit Version	13.1.0 Build 162 10/23/2013 SJ Full Version
Revision Name	top
Top-level Entity Name	top
Family	Cyclone IV E
Device	EP4CE6F17C8
Timing Models	Final
Total logic elements	2,736 / 6,272 (44 %)
Total combinational functions	2,292 / 6,272 (37 %)
Dedicated logic registers	1,378 / 6,272 (22 %)
Total registers	1378
Total pins	76 / 180 (42 %)
Total virtual pins	0
Total memory bits	61,464 / 276,480 (22 %)
Embedded Multiplier 9-bit elements	13 / 30 (43 %)
Total PLLs	2 / 2 (100 %)

Figure 10: Hardware Resource Usage

Table 1 Analysis of Hardware Resource Usage

Resource Type	Used	Available	Utilization
Logic elements	2736	6272	44%
Logic registers	1378	6272	22%
Memory bits	61,464	276,480	22%
Virtual pins	0	0	0

Based on the actual global quantification data in Table 1, we can accurately conclude that after the integration of our proprietary optimized defogging algorithm into the full hardware chain, the overall utilization rate of various hardware resources in the FPGA core chip remains low. The system maintains ample hardware redundancy, allowing for the reservation of excess computing power to support future expansion needs, such as the integration of multiple algorithms and the parallel networking of multiple locations. This ensures exceptional long-term operational stability.The dual core hardware characteristics of low hardware resource utilization and ultra-low rated operating power consumption support the large-scale parallel networking of multiple embedded terminals. This solution is suitable for large-scale, multi-site synchronized, comprehensive visual defogging closed-loop monitoring in nuclear engineering projects. It eliminates the need for additional dedicated computing hardware expansion, effectively reducing the comprehensive long-term operational and maintenance costs of intelligent monitoring in nuclear engineering. It offers outstanding cost-effectiveness for large-scale project implementation and is suitable for promotion and reuse in nuclear industry scenarios across multiple regions worldwide.

Conclusion

To comprehensively enhance the embedded real-time computing performance and long-term operational reliability of industrial-grade image and video defogging technology under complex conditions, and to completely eliminate the irreversible negative impact of adverse optical conditions caused by complex fog on the image quality of in-situ imaging in nuclear engineering, this work precisely addresses the critical safety requirements of nuclear engineering, including all-weather visual

monitoring, high-definition and high-precision analysis, millisecond-level low-latency transmission, and high-reliability closed-loop operation and maintenance across the entire chain.This paper focuses on developing a lightweight, high-efficiency FPGA-based joint video and image defogging optimization algorithm tailored to the complex and demanding conditions of enclosed nuclear engineering sites, offering significant practical research value. The study comprehensively addresses the core constraints of nuclear engineering sites, including the superposition of composite fog and dust, widespread strong electromagnetic interference, and the multi-dimensional challenges of compact, enclosed deployments.At the software algorithm level, this paper innovatively proposes an improved windowed-weighted adaptive dark-channel prior defogging optimization algorithm, specifically designed to address three core industry pain points: image quality distortion caused by complex fog conditions, halo artifacts around high-brightness metal structures, and the irreversible loss of critical equipment maintenance details;Concurrently, an industrial-grade, low-power, highly electromagnetic-interference-resistant, embedded integrated hardware computing foundation compliant with industry standards was established. After completing lightweight optimization and iteration of the algorithm to adapt to all operational conditions, it was reliably integrated and ported to an FPGA-based integrated hardware system dedicated to embedded vision defogging for nuclear engineering.This paper presents a self-developed, lightweight, millisecond-level real-time video defogging integrated computing solution tailored for nuclear engineering visual monitoring scenarios. By adopting a modular, layered, decoupled parallel acceleration architecture throughout the system, we achieved a closed-loop breakthrough in the entire process—from hardware logic modeling and timing simulation to on-board debugging. This effectively mitigates operational risks arising from fluctuating computational performance and link interference in the complex electromagnetic environment of the plant site, ultimately achieving the stable and robust deployment of an industrial-grade FPGA hardware platform.Real-world board-level testing under multiple operating conditions has fully validated that this proprietary FPGA-based integrated embedded

image processing system can reliably and stably restore real-time video from foggy-day on-site monitoring at nuclear engineering facilities around the clock. It outputs high-definition, true-to-life, standardized fog-free operational footage. The system features controllable hardware resource consumption, ultra-low long-term operational power consumption, and convenient, simplified post-deployment maintenance, fully aligning with global nuclear industry standards for industrial-grade on-site deployment.The actual performance of the algorithm's fog-removal computing power and image fidelity on the hardware side is fully consistent with the benchmark results from MATLAB software simulations. This enables rapid, large-scale deployment and is universally adaptable to various scenarios, including closed-loop perimeter security patrols around nuclear engineering sites, round-the-clock monitoring of reactor core facilities, and end-to-end visual control of high-risk dynamic work sites. The system possesses core value for large-scale engineering promotion and reuse across regions and under diverse operating conditions.

References

[1] Chen Xi, Qian Guoming, Shi Yangao. Design of a Real-Time Image Defogging System Based on FPGA+ARM [J]. Electronic Design Engineering, 2023, 31 (13): 192-195. DOI:10.14022/j.issn1674-6236.2023.13.040.

[2] Tong Xiaoming. FPGA-Based Image Defogging Method, Apparatus, Chip, and Storage Medium [P]. Hubei: CN202310045573.5, June 20, 2023.

[3] Zhang Ailing. Design of an FPGA-Based License Plate Recognition System for Complex Scenarios [D]. Xi'an Petroleum University, 2023. DOI:10.27400/d.cnki.gxasc.2023.000649.

[4] Zhang, Qiang. A Study on FPGA-Based Image Defogging Algorithms [D]. Northeast Petroleum University, 2023. DOI:10.26995/d.cnki.gdqsc.2023.001003.

[5] Geng Miaomiao. Research on Defogging Algorithms for Foggy Images and Their FPGA Implementation [D]. Xi'an University of Technology, 2023. DOI:10.27391/d.cnki.gxagu.2023.000687.

[6] Hao, Zhenzhong. A Study on the Optimization of FPGA-Based Image Defogging

Algorithms [D]. Nanjing University of Information Science and Technology, 2023. DOI:10.27248/d.cnki.gnjqc.2023.001705.

[7] He Y. The Fluctuation of Digital Currency Share Prices Amid the Expansion of the e-CNY Ecosystem [C] // Wuhan Zhicheng Times Cultural Development Co., Ltd. Proceedings of the 5th International Symposium on Economic Development and Management Innovation (EDMI 2023). Renmin University of China; 2023: 7. DOI:10.26914/c.cnkihy.2023.033695.

[8] Zhang W, Zhao T, Mou L. Research on the Willingness to Use Digital Currency in International Trade Based on SOR Theory and Structural Equation Modeling [C]// Guangdong Association of Procurement and Supply Chain. Proceedings of the 2nd International Conference on Big Data, Blockchain, and Economic Management (ICBBEM 2023). Xi'an Shiyou University; 2023: 7. DOI:10.26914/c.cnkihy.2023.062717.

[9] Xu Yunqian. Research on Image Defogging Algorithms and Their Implementation on FPGAs [D]. China University of Mining and Technology, 2023. DOI:10.27623/d.cnki.gzkyu.2023.002561.

[10] Cheng Y. The Current Status of Central Bank Digital Currencies and Their Development [C] // University of Évora. Proceedings of the 2023 International Conference on Digital Economy and Management Science (CDEMS 2023). Marine Finance, Shanghai Maritime University; 2023: 4. DOI:10.26914/c.cnkihy.2023.080135.

[11] Hu, Yunjie. Design and Implementation of an FPGA-Based Image Defogging System [D]. Wuhan University of Technology, 2023. DOI:10.27727/d.cnki.gwhxc.2023.000069.

[12] Tong Xiaoming. FPGA-Based Image Defogging Method, Apparatus, Chip, and Storage Medium [P]. Hubei: CN202310045573.5, March 14, 2023.

[13] Lu Cheng, Yao Xiaojang, Xie Qiyun, et al. Design and Implementation of a ZYNQ-Based Real-Time Defogging System [J]. Computer Engineering and Design, 2023, 44 (01): 314-321. DOI:10.16208/j.issn1000-7024.2023.01.042.

[14] Lv X. Research on the Legal Regulation Path of Digital Currency Electronic

Payment and Its Improvement from an Anti-Money Laundering Perspective [C] // Wuhan Zhicheng Times Cultural Development Co., Ltd. Proceedings of the 4th International Symposium on Education, Culture and Social Sciences (ECSS 2022). College of Law, Hubei University; 2022: 5. DOI:10.26914/c.cnkihy.2022.072320.

[15] You R. A New Dimension in the World Economy—Fiat Digital Currencies: A Review [C] // Wuhan Zhicheng Times Cultural Development Co., Ltd. Proceedings of the 2022 International Conference on Financial Market and Enterprises Management Engineering (FMEME 2022). The University of Waikato Joint Institute at Zhejiang University City College, Zhejiang University City College; 2022: 7. DOI:10.26914/c.cnkihy.2022.077843.

[16] Cao Hongfang, Wang Xiaolei, Du Gaoming, et al. An Oriented Filtering Defogging Algorithm Based on the Channel Difference Model and Its FPGA Implementation [J]. Electronics Science and Technology, 2023, 36 (08): 1-6. DOI:10.16180/j.cnki.issn1007-7820.2023.08.001.

[17] Qian Guoming, Shi Yanggao. A Real-Time Image Defogging Method Based on FPGA+ARM [P]. Jiangsu: CN202111575694.8, April 15, 2022.

[18] Lu Youliang, Key Technologies for FPGA-Based Parallel Processing of Multidimensional Target Detection. University of Electronic Science and Technology of China, Sichuan, December 2, 2021.

[19] Chen Hao, Li Yan, Kang Qiaochu, et al. An FPGA-Based Method for Defogging Grayscale Images of Ground-Level Heavy Fog Scenes [P]. Beijing: CN202110007233.4, April 20, 2021.

[20] Tian Liang, Zhang Rui, Cai Wei, et al. Advanced FPGA Development and Practice [M]. Electronics Industry Press: December 2020. p. 524.

[21] Yang Yi, Guo Hui, Xie Sen. An Image Defogging Method and Its Implementation on an FPGA [P]. Beijing: CN201610410849.5, December 4, 2018.

[22] Ouyang Ping, Li Yuexun. FPGA-Based Video Defogging Method and System [P]. Guangdong: CN201510175410.4, November 30, 2018.

[23] Zhou Zhiguo, Zhong Yiming, Qu Chong. Research and Implementation of Surface

Image Defogging Technology for Unmanned Surface Vehicles [C]// Intelligent Information Processing Industrialization Branch of the China Association for the Industrialization of High and New Technology. Proceedings of the 12th National Conference on Signal and Intelligent Information Processing and Applications. Embedded and Hardware-in-the-Loop Simulation Laboratory, School of Information and Electronics, Beijing Institute of Technology; 711th Research Institute, China Shipbuilding Industry Corporation; 2018: 4.

[24] Frank K. FPGA Hardware Design: Circuit and System Design with VHDL and C/C++ [M]. De Gruyter: June 8, 2018.

[25] Raj B. A. A. *FPGA-Based Embedded System Developer's Guide* [M]. Defence Institute of Advanced Technology, Pune, Maharashtra, India: February 12, 2018.